drothermal synthesis a solid black spongy block was obtained at the bottom of the autoclave, Figure 3.23 b, showing a drastic change in color compared to the staring dispersion, which is usually indicative of GO reduction and increase of hydrophobicity, with an unavoidable random aggregation of the sheets due to the removal of the oxygen functionalities (101). The typical self-assembled hydrogels reported previously were usually constructed by self-assembling small molecules or macromolecules to form networks with physical cross-links (115), (116).

The cylindric graphene hydrogel has a diameter of about 1 cm and it is strong enough to

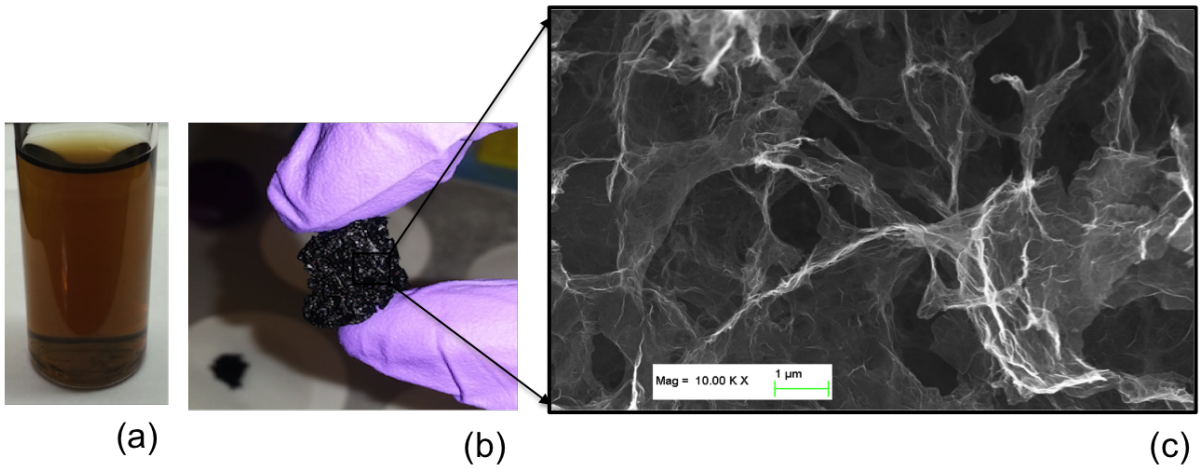

Figure 3.23 Photograph of the GO/DI water dispersion (a); reduced graphene oxide hydrogel obtained from the hydrothermal synthesis (b) and FESEM showing its porous structure (c).

support a 40 g weight with little deformation, see Figure 3.24, behaving like an elastic-plastic foam under compression (117). The structure obtained is a well-defined and interconnected

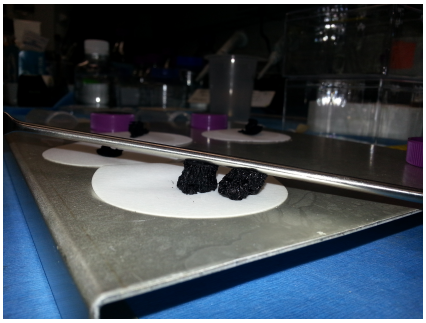

Figure 3.24 Picture of the hydrogels with a spatula on top.

3D porous network. The properties of the porous block strongly depend on GO concentration and hydrothermal reaction time. When the concentration was low (e.g., 0.5 mg/ml), only a black powdery material was produced after 12 h hydrothermal reduction, and this result is consistent with that of a previous report (94). However, as the concentration was increased to 1 or 2 mg/ml, more mechanically stable samples were obtained (114).

GO sheets during hydrothermal reduction can induce partial overlapping or coalescing of flexible graphene sheets via π-π stacking interactions, which forms the strong cross-links of the 3D graphene network as demonstrated by FESEM analysis of the synthesized material, showed in Figure 3.23 c. Weak bonding interactions such as van der Waals force, hydrogen bonding, stacking, and inclusion interaction are established among graphene sheets, forming high surface area porous structures with macro-, meso-, and micro-pores that are ideal for electrochemical purposes favoring the ionic insertion. The pore sizes of the network are in the range of submicrometer to several micrometers and the pore walls consist of thin layers of stacked graphene sheets.BrunauerEmmettTeller (BET) analysis was conducted on the samples obtained after the freeze dry process and a surface area of about 1400 m^2/g was obtained with a pore volume of 1.08 cc/g and micropore volume of 0.2 cc/g. This is mainly due to the recovery of conjugated system from GO sheets upon hydrothermal reduction, thanks to these residual hydrophilic oxygenated groups, the reduced GO sheets can encapsulate water in the process of self-assembly.

In order to verify the reduction of the graphene oxide due to the hydrothermal synthesis XPS characterization was performed on the sample before and after the process. The XPS spectra are reported in Figure 3.25. The removal of oxygen functionalities from GO sheets is confirmed analyzing the intensities of the deconvolution peaks, that for the rGO samples the reduction of intensity of C=O (carbonyl), and C-O (epoxy/alkoxy) and the disappearance of the groups O-C-O (epoxide) compared to the GO C1s XPS spectrum (91), (103). The C/O ratio content significantly increases after the hydrothermal treatment (94), (114) and (170), as indicated by the analysis of XPS peak area ratios for different oxygen functionalities towards C-C bond, summarized in Table 3.5.

X-Ray diffraction characterization reported in Figure 3.26, shows that the graphene porous structure diffraction peak is broader compared with the graphite and graphene oxide ones,

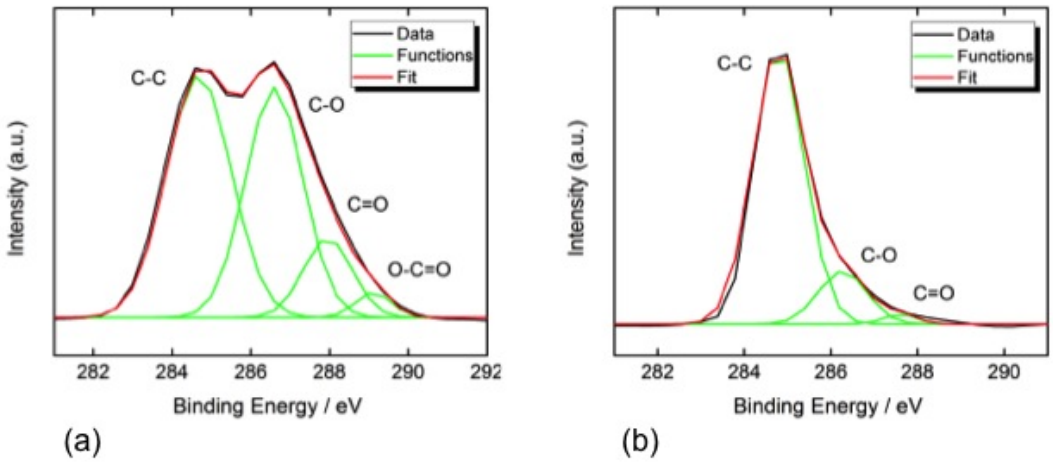

Figure 3.25 XPS spectra of a) Graphene oxide and b) reduced graphene oxide after hydrothermal synthesis

Table 3.5 XPS peak area C/O ratios for different functional groups of GO and rGO

Sample	**C-C/C-O**	**C-C/C=O**
GO	0.9	3.8
rGO	3.8	13.9

indicating the poor ordering of graphene sheets along their stacking direction and that the framework of the graphene porous structure is composed of few-layer stacked graphene sheets (114), (170). The pattern of graphene porous structure exhibits a broad peak centered at 2θ = 18.3 corresponding to the graphitic profile with an interlayer spacing of 3.77 Å. This value is much smaller than that of the GO precursor (6.94 Å), while still being higher than that of graphite (3.36 Å). This result suggests the recovery of π–conjugated structure from GO sheets upon hydrothermal reduction and also the presence of residual oxygenated functional groups on reduced GO sheets (220).

Raman spectra of GO starting material and rGO hydrogel have been also performed and are reported in Figure 3.27. The spectra present the typical G, D and 2D peaks of the carbon based material (86), and an important information is the increase of the relative intensity of the ratio I_D/I_G that means that an increase of the disorder degree in the material is occurring due to the reduction process during the hydrothermal synthesis. In fact, it is possible to think that

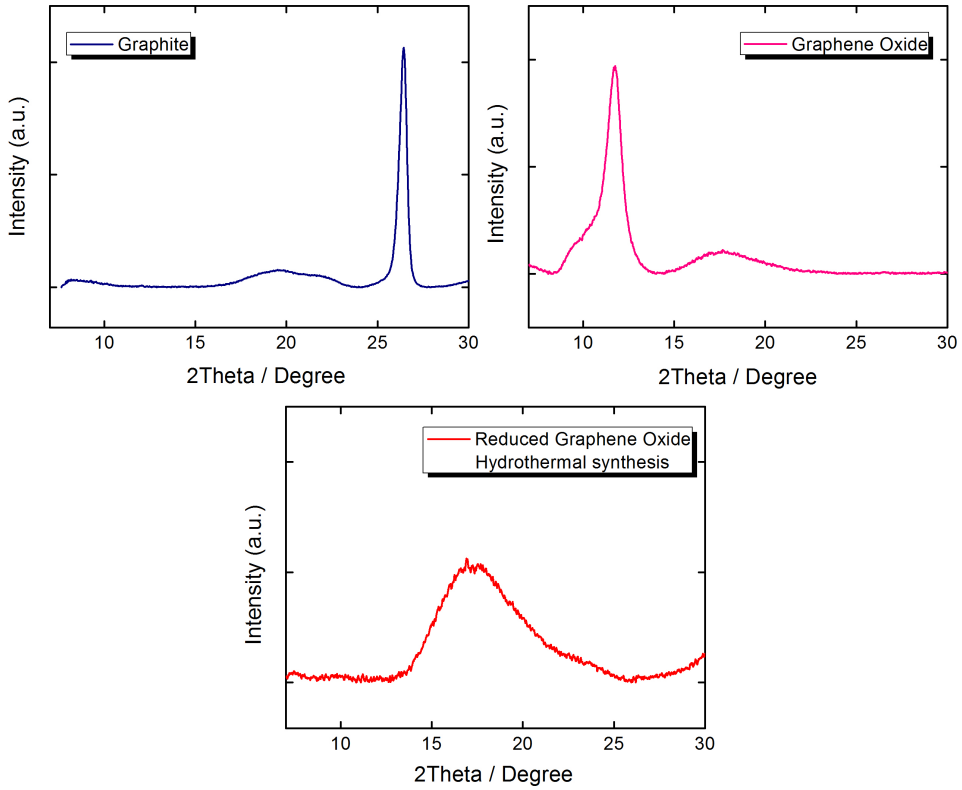

Figure 3.26 X-Ray Diffraction spectra of expanded graphite (blue), graphene oxide (pink) and reduced graphene oxide with hydrothermal synthesis (red).

damages in the atomic structure can be introduced from the mechanical interaction between the sheets in the autoclave at high temperature and pressure.

The high thermal stability of the 3D structured graphene is another interesting and important property for future applications (114), and for this reason thermo gravimetric analysis (TGA), reported in Figure 5.11, was also performed on the hydrothermal reduced graphene oxide and was verified that it can tolerate high temperatures of approximately 450^{o}C, measuring in air with a ramp of 5 degree per minute.

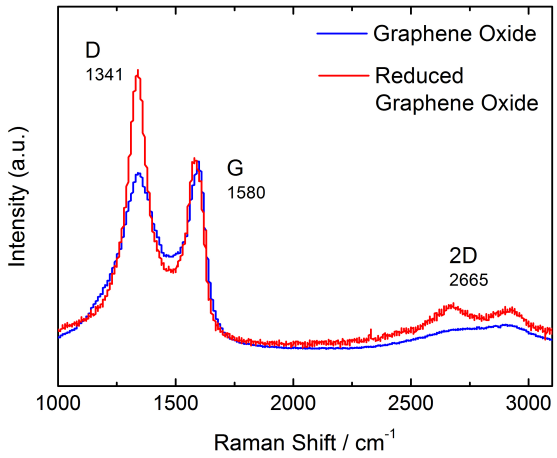

Figure 3.27 Raman spectroscopy data comparing the commercial graphene oxide (blue line) and reduced graphene oxide (red line).

3.3 Conclusion

In conclusion, three different reduction methods for the graphene oxide have been verified and discussed. All three methods are efficient and the reduction of the graphene oxide is achieved by using environmentally friendly, low power consumption and low cost processes. The characteristics of these methods are interesting and they can have interesting applications for the fabrication process of graphene based composite materials, that can be used in different fields. In the next chapters are going to be explored two possible applications of the reduced graphene oxide. UV-light, hydrothermal and chemical graphene oxide reduction are respectively employed in fabrication process for flexible electronics and energy storage devices applications.